



**Acoustics'08
Paris**
June 29-July 4, 2008

www.acoustics08-paris.org

High-frequency multibeam echosounder classification for rapid environmental assessment

Kerstin Siemes^a, Mirjam Snellen^a, Dick Simons^b, Jean-Pierre Hermand^c,
Matthias Meyer^{d,c} and Jean-Claude Le Gac^e

^aAcoustic Remote Sensing Group, Delft Institute of Earth Observation and Space Systems,
Delft University of Technology, Kluyverweg 1, 2629 HS Delft, Netherlands

^bDelft University of Technology, P.O. Box Postbus 5048, 2600 GA Delft, Netherlands

^cUniversité libre de Bruxelles (U.L.B.) - Environmental hydroacoustics lab, av. Franklin D.
Roosevelt 50, CP 194/5, 1050 Bruxelles, Belgium

^dRoyal Netherlands Naval College (NLDA) - REA group, PO Box 10000, 1780 Den Helder,
Netherlands

^eNATO Undersea Research Center, Viale San Bartolomeo 400, 19126 La Spezia, Italy
k.siemes@tudelft.nl

For shallow water naval operations, obtaining rapidly an accurate picture of the environmental circumstances often is of high importance. The required information typically concerns water column properties, sea surface roughness, and sediment geo-acoustic properties. Hereto a multi-sensor approach is required. In this context, the BP'07 experiment has been carried out south of Elba (Mediterranean Sea), where several techniques of environmental characterization have been combined. A part of BP'07 was dedicated to measurements carried out with a multibeam echosounder. This system provides depth information, but also allows for seafloor classification. The classification approach taken is model-based employing the backscatter data. It discriminates between sediments in the most optimal way by applying the Bayes decision rule for multiple hypotheses, implicitly accounting for ping-to-ping variability in backscatter strength. For validating the resulting geo-acoustic estimates sediment samples were collected. Here, besides the analysis of the depth measurements, the results of the seafloor classification using the multibeam data and a preliminary comparison with the sediment sample analysis are presented.

1 Introduction

Coastal shallow water regions cover an area of approximately $3 \times 10^7 \text{ km}^2$ [5] and are characterized by a high variability in sediment composition. Further, these regions become more and more stage of human interaction with the seabottom. Rapid determination of the sediment composition is therefore requested in many disciplines. For example, the impact of building offshore wind turbines on the sediment has to be controlled or areas consisting of a special sediment type need to be detected.

As bottom grabbing is very time consuming (about 30 grabs of $0.1 - 0.2 \text{ m}^2$ can be taken per day [10]) and necessitates laboratory analysis afterwards this method is not suited for rapid environmental assessment. Employing multibeam echosounders (MBES) promises to be a suited alternative.

This article is based on the multidisciplinary BP'07 (battlespace preparation 2007) experiment described in [7] that was carried out by several vessels in the Mediterranean Sea south-east of Elba Island in 2007. Data analysed here were collected during 12 days (23 April - 4 May) from the Dutch HNLMS Snellius. Results presented in this article are focused on MBES measurements and bottom grabs taken during this period. From the MBES, information on the bathymetry and backscattering values can be obtained. The aim is to use these data for seabottom classification, i.e. obtaining information about the geo-acoustic properties. Additionally, bottom grabs are used for ground-truthing. In section 2 a brief description of the research area and the equipment of the ship is given. After having calculated the bathymetry of the MBES's depth data in section 3, seafloor sediments are classified by a Bayesian approach using backscatter strength values in section 4. The next step is the comparison with groundtruthing data. An analysis of the bottom grabs taken in the research area is presented in section 5. Finally results are summarized and embedded in the context of the whole research project in section 6.

2 Experimental Settings

2.1 Research Area

Measurements took place south-east of Elba Island. An overview of the experimental area is given in figure 1.



Figure 1: Overview of the BP'07 reasearch area (<http://maps.google.de>).

Coordinates of the research area in the system of WGS84 lie coarsly between 10.6 deg and 11.0 deg eastern longitude and 42.55 deg and 42.8 deg northern latitude, covering an area of 33 km by 28 km. In this shallow water area of the continental shelf, depths reach 10 m to maximal 160 m. Shallowest are the regions near to the coast of Italy in the north-eastern part of the research area.

2.2 Instrumentation

Mounted on board of HNLMS Snellius was a SIMRAD EM3000D dual head MBES operating at 300 kHz. This sonar has an opening angle of 130 deg and covers therefore a swath between 40 m and 1000 m (dependent on the water depth which lies in between 10 m and 200 m) when assuming a horizontal flat bottom. Along this swath 254 beams are formed.

Data are provided in a binary raw-format. These raw-files include different types of datagrams, containing different variables. For our purpose we are interested in the depth and backscatter values.

Unfortunately, no positions are recorded with this system. We obtain navigation data from GPS measurements that were stored with singlebeam echosounder data. Via time comparison positions can be added to the MBES data.

Also on board was a Hamon grabber [7] for taking grab samples of the upper seabottom sediments. Along the whole track 24 bottom grabs of about 20 cm depth were taken with this instrument.

3 Bathymetry measurements

Bathymetry is obtained from the two-way travel time as measured by the MBES for each beam and the sound velocity profile in seawater.

As sound velocity in the water column determines the behavior of sound propagation [1] it plays an important role in measuring the range of every beam. Two ways of accounting for the sound velocity profile are discussed in the following. We will compare the more time consuming common ray tracing method and an approach suggested by Geng and Zielinski [2] using an equivalent linear sound velocity profile.

3.1 Ray tracing for depth error correction

Let us consider a sound velocity profile consisting of multiple (n) linear segments as shown in figure 2. The ray tracing approach calculates step-by-step the changes in angle and position of the sound ray at each depth at which a change in sound velocity occurs. Starting with angle θ_0 we can derive the angles at the other depths via Snell's law

$$\frac{\cos \theta_0}{c_0} = \frac{\cos \theta_m}{c_m}, \text{ for } m \in \{1, \dots, n\} \quad (1)$$

The position of the sound ray at the lower end of the m -th segment can be calculated as follows.

$$x_m = x_{m-1} + R_m \cdot (\sin(\theta_m) - \sin(\theta_{m-1})); \quad (2)$$

$$z_m = z_{m-1} + |R_m \cdot (\cos(\theta_{m-1}) - \cos(\theta_m))|; \quad (3)$$

Here, x_{m-1} , x_m denote the across track positions and z_{m-1} , z_m the depth values at the upper and lower end of the m -th segment respectively. And R_m is the radius of the sound ray in the segment m .

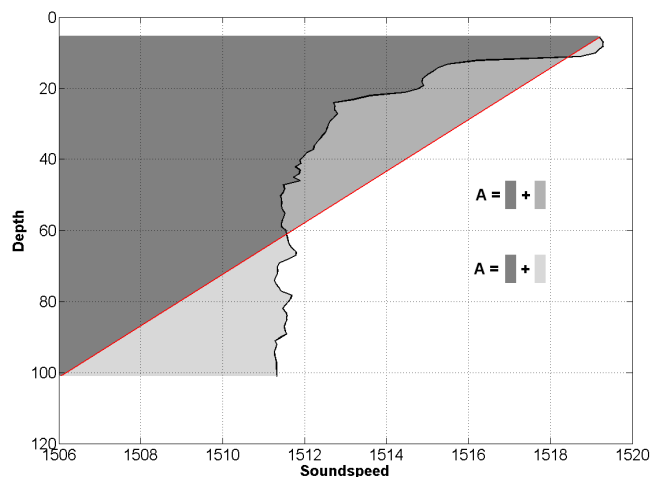


Figure 2: Sound velocity profile consisting of multiple linear segments taken at 42.37 N and 10.49 S versus equivalent linear profile.

3.2 Equivalent linear profile

Again we start with a sound velocity profile consisting of multiple linear segments. As the ray tracing method

is very time consuming, especially for sound velocity profiles with a large amount of segments, it would be an advantage to reduce the number of segments without reducing the accuracy. Reference [2] introduced an approach that makes use of simple linear sound velocity profiles, containing only one segment. According to [2], the position at which sound impings on the seafloor is almost the same for a family of sound velocity profiles. Such a family contains all sound velocity profiles that include the same area between the profile and the depth-axis.

The starting point (z_0, c_0) of the profile stays the same as in the ray tracing approach. The soundspeed c_n at the endpoint of the profile results from the the area A under the original profile and the known depth z_n of the profile and is given as

$$c_n = 2 \cdot \frac{A}{z_n - z_0}. \quad (4)$$

In this way the area under the original and the new profile are equal as shown in figure 2.

3.3 Results

Depth values have been corrected for refraction according to the ray tracing approach as well as the approach which uses a linear profile. A comparison is shown in figure 3.

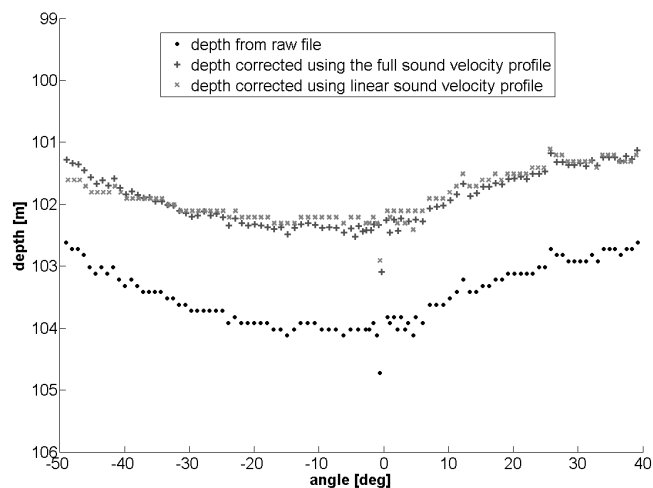


Figure 3: Depth along a swath at a deeper part of the research area at different stages of analysis: uncorrected raw data and depth with refraction correction (full profile and linearized profile).

It is seen that both approaches give almost the same results, indicating the applicability of the approach described in section 3.2. At depths of about 100 m, errors of 2 m occur when not accounting for refraction. In the shallower parts we do not notice remarkable differences in the depth values, whether we account for changes in sound velocity or not.

4 Seabed classification by means of backscatter values

Besides depth information as discussed in section 3 the MBES provides the backscatter strength of the received signal. According to the properties of the seabottom like roughness and hardness the backscatter strength varies with the sediment type. In this section we make use of backscatter strength values to classify the seabed of the BP'07 research area. The classification technique is described in section 4.1. We apply a Bayesian approach as suggested by [9]. Resulting classes are presented in section 4.2. Note that these classes still do not give any information about the sediment types that can be found in the research area. Determining sediment types from observed backscatter strength requires ground truth values e.g. taken by grabbing as discussed in section 5.

4.1 Classification technique

The parameter we use for seabottom classification is the averaged backscatter strength BS_θ per beam. Let N_θ be the number of scatter pixels over which the averaging is performed. The averaged backscatter strength in decibel (dB) unit follows from backscatter intensity I_θ as

$$BS_\theta = \frac{1}{N_\theta} \sum_{n=1}^{N_\theta} 10 \log_{10} I_\theta. \quad (5)$$

Assuming I_θ is exponentially distributed and single backscatter values are assumed to be independent, BS_θ becomes normally distributed for large N_θ . Therefore, we fit a model $f(BS_\theta|x)$ existing of a sum of scaled Gaussians to the histogram of observed backscatter values BS_θ .

$$f(BS_\theta|x) = \sum_{k=1}^m c_k \exp\left(-\frac{(BS_\theta - \mu_{\theta k})^2}{2\sigma_{\theta k}^2}\right) \quad (6)$$

Parameters to be estimated are the scaling factor c_k and the mean $\mu_{\theta k}$ and standard deviation $\sigma_{\theta k}$ of each Gaussian probability density function (PDF). These are contained in the factor x . The number of Gaussians employed is equal to the (unknown) number of seabottom types.

First of all the number of classes has to be determined iteratively. Starting with one curve the number of Gaussians step-by-step is increased by one. A reduced χ^2 -statistic helps us to decide on the goodness of fit. The iteration is stopped if the reduced χ^2 value falls below a critical value. The number of classes will be m after the m -th step.

Once the number of classes is known, classification is done by applying the Bayes criterion for decision. According to the number of classes m simple hypotheses H_1, \dots, H_m can be set up. $H_j : x = x_j$ is the hypothesis that for a backscatter value BS_θ the parameter set x_j is the one to choose. Bayes' rule gives the a-posteriori probabilities $P(x_j|BS_\theta)$ for observed BS_θ .

$$P(x_j|BS_\theta) = \frac{f_\theta(BS_\theta|x_j)P(x_j)}{f_\theta(BS_\theta)} \quad (7)$$

with $P(x_j) = \frac{1}{m}$ denoting the a priori probability, where we assume all seafloor types a priori to be equally likely.

Therefore, using a 'maximum a-posteriori' probability criterion we have to accept the hypothesis H_j if the following is valid (i.e. we choose for the class which is most likely):

$$\max\{f_\theta(BS_\theta|x_k)P(x_k)\} = f_\theta(BS_\theta|x_j)P(x_j) \quad (8)$$

with $k = 1, \dots, m$

The acceptance region of a hypothesis is determined by the intersection of its Gaussian curve with the neighbouring Gaussians.

4.2 Results

Backscatter values are analyzed per angle. Basically we are interested in lower grazing angles since beams at these angles cover a larger beam footprint. This provides results in the shallower parts of the research area only. To get an overview over the whole area we have to extend our analysis to angles up to 40° .

To avoid large overlapping of the Gaussian curves and therefore reducing β , we restricted the number of classes to three. The result of a Gaussian fit is shown in Fig. 4.

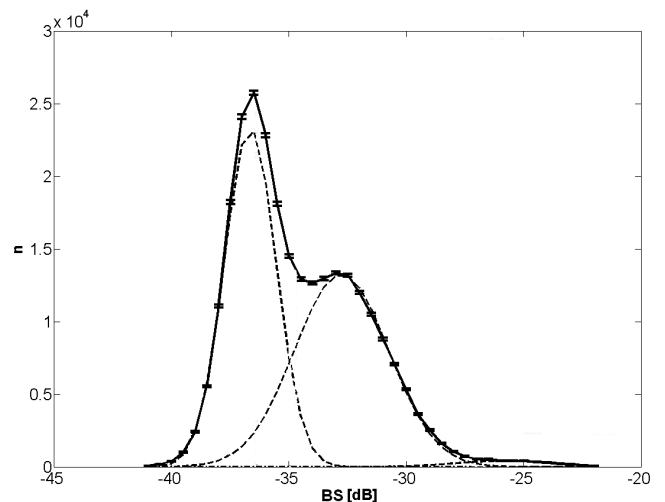


Figure 4: Fit of Gaussians (dashed) to the PDF of the backscatter values BS_θ .

Class boundaries are defined by the intersection of the Gaussians. Fig. 5 shows these intersection points. Also indicated in this figure are probabilities of incorrect decisions, i.e. β_{12} is the probability that H_1 is accepted, whereas actually H_2 holds. And β_{21} is the probability that H_1 is accepted, whereas actually H_2 holds.

However, we find values for β_{21} up to 14%. Hence we introduce 'mixed' classes to weaken the strict boundaries and absorb statistical fluctuations. New boundaries were set at those points where β is 1%. Note that a 'mixed' class not necessarily means a new seafloor type. This approach results in a backscatter map depicted in Fig. 6. 'Mixed' classes are not shown in this figure. An increase in backscatter strength can mainly be observed from the coast to the deeper parts of the research area. The obtained classes run nearly parallel to the coastline.

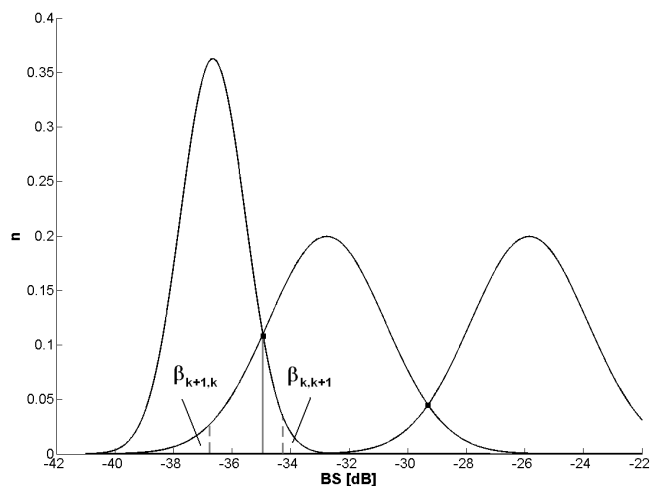


Figure 5: Normalized Gaussians and probabilities of incorrect decisions. The solid line gives one of the class boundaries when not allowing for 'mixed' classes. The dashed lines indicate 'mixed' classes.

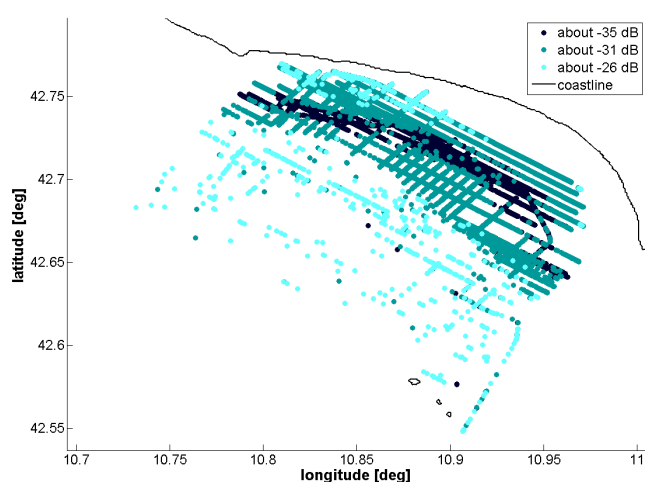


Figure 6: Classification results at 34° grazing angle. The three obtained classes have a mean value of -35 , -31 , -26 dB respectively and run nearly parallel to the coastline.

5 Bottom grab analysis for ground truthing

During the BP'07 experiment 24 bottom grabs were taken with a Hamon grabber to provide ground truth data. Ground truthing is necessary to find the relationship between sediment types and classes of backscatter strength values from the MBES data.

These bottom grabs were analyzed at TNO, the Netherlands where they were dried, sieved with different sized sieves and sorted by grain size. Documented is information about the minimum (D_{min}), maximum (D_{max}) and average (D) diameter of the sediment particles in micrometer units as well as the particle size in ϕ -units. The particle size (d) in ϕ -units results from the (average) grain diameter in millimeter according to

$$d = -\log_2 D. \quad (9)$$

The core results shown in this section are comparable to those of the upper sediment layers of core samples taken in the research area at former experiments, which are described in [3] and [4].

5.1 Classification of bottom grab sediments

The classification of bottom grab sediments based on the Wentworth scale [11] is shown table 1.

maximum diameter [mm]	sediment
2	very coarse sand
1	coarse sand
1/2	medium sand
1/4	fine sand
1/8	very fine sand
1/16	silt
1/256	clay

Table 1: Wentworth scale of sediment sizes.

In most parts of the research area clay is the dominating sediment type, amounting to 60 – 70%. Only near to the coast in the north-eastern part somewhat coarser sediments occur and the silt fraction increases up to 40–60%. Additionally, for these grabs even 5% sand has been found. It is to be said that the sum of all mass frequencies does not reach 100% because the analysis method did not account for sediments smaller than 1 micrometer.

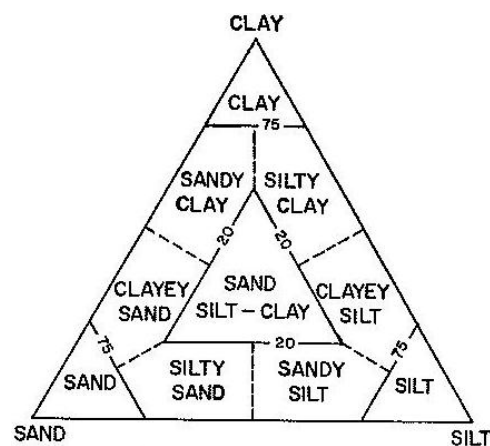


Figure 7: Sediment types of finer sediments as introduced by Shepard. Sediments are differentiated by their relative composition of sand, silt and clay [6].

To get a finer differentiation of the silt and clay types, we will now consider sediment classes as introduced by Shepard in 1954 [8]. They are obtained from the relative proportion of sand, silt and clay. Fig. 7 shows Shepard's 10 different classes of finer sediments. From the shallower coastal area to the deeper part (up to 200m) the sediment composition changes from clayey silt (the coarsest sediment in this area) over silty clay to clay (see Fig. 8).

Another approach in addition to the Wentworth classification employs mean grain size values in ϕ -units and attains similar results. The mean grain size is calculated from

$$M_z = \frac{d_{16} + d_{50} + d_{84}}{3} \quad (10)$$

with d_x denoting the grain size (in ϕ -unit) at which $x\%$ of the sediments in the sample are smaller. In Fig. 8 we also see a gradient in grain size from the coast to the deeper regions. Mean grain sizes do not reach values below 7ϕ . According to Eq. 9 this means we are only dealing with grain sizes less than 8 micrometer.

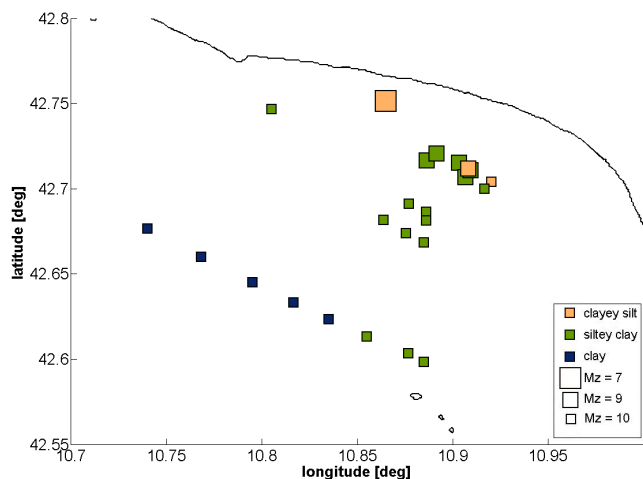


Figure 8: Position of bottom grabs and occurring sediments. Mean grain size is illustrated in the marker size while color represent Shepard's classes clayey silt, silty clay and clay. In deeper parts of the research area clay is been found. Closer to the coast, slightly coarser sediments with $M_z = 7\phi$ can be found.

5.2 Comparison of sediment types and backscatter values

Analysis of backscatter strength and sediment composition show comparable pictures of seabottom classes. In both cases, backscatter analysis and bottom grab analysis, the classes run nearly parallel to the coastline with a gradient towards the deeper parts of the research area. Curiously, about 10 dB larger backscatter values occur at sediments with smaller grain size. Increased volume scattering in the clayey bottoms can be responsible for this phenomenon.

6 Summary and future research

Our long-term objective is to obtain rapidly an accurate picture of the environmental circumstances which accumulate bathymetric and sedimentary information. By now bathymetry has been recalculated accounting for watercolumn sound velocity profiles.

With regards to classification aspects, we are able to detect classes of backscatter strength per beam with a Bayesian approach. A comparison with groundtruth data gives promising results for detecting grain sizes up

to 9ϕ . The next step to be done is the combination of classification results from different angles. Further, aspects of bathymetry can be taken into account as new features in the classification. That is for example slope, which could influence the occurrence of specific sediment types.

References

- [1] P.C. Etter. *Underwater Acoustic Modelling and Simulation*. Spon, 3 edition, 2003.
- [2] X. Geng and A. Zielinski. Precise Multibeam Acoustic Bathymetry. *Marine Geodesy*, 28(2):157–167, 1999.
- [3] J.-P. Hermand. Broad-Band Geoacoustic Inversion in Shallow Water from Waveguide Impulse Response Measurements on a Single Hydrophone: Theory and Experimental Results. *IEEE Journal of Oceanic Engineering*, 24(1):41–66, 1999.
- [4] J.-P. Hermand and P. Gerstoft. Inversion of Broad-Band Multitone Acoustic Data from the YELLOW SHARK Summer Experiments. *IEEE Journal of Oceanic Engineering*, 21(4):324–346, 1996.
- [5] D.R. Jackson and M.D. Richardson. *High-Frequency Seafloor Acoustics*. Springer, 2007.
- [6] W.C. Krumbein and L.L. Sloss. *Stratigraphy and Sedimentation*. Freeman, 2 edition, 1963.
- [7] J.-C. Le Gac and J.-P. Hermand. NURC - a NATO Research Centre BP'07 Cruise Report, 2007.
- [8] F.P. Shepard. Nomenclature based on sand-silt-clay ratios. *Journal of Sedimentary Petrology*, 24:151–158, 1954.
- [9] D.G. Simons and M. Snellen. A bayesian approach to seafloor classification using multi-beam backscatter data. *Applied Acoustics, under review*, 2008.
- [10] N.S. Thomas. Procedural Guideline No. 3-9 Quantitative sampling of sublittoral sediment biotopes and species using remote-operated grabs.
- [11] C.K. Wentworth. A scale of grade and class terms for clastic sediments. *Journal of Geology*, 30:377–392, 1922.